# Strength and Microstructural Characteristics of Flyash-Waste Glass Powders Ternary Blended Concrete

Moruf O. Yusuf * , Khaled A. Alawi Al-Sodani , Adeshina A. Adewumi , Muyideen Abdulkareem , Ali H. AlAteah

Posted Date: 22 August 2025

doi: 10.20944/preprints202508.1648.v1

Keywords: waste glass; admixtures; microstructures; construction materials; fly ash/ slags; high strength concrete

 doi:10.20944/preprints202508.1648.v1



*Article*

# Strength and Microstructural Characteristics of Flyash-Waste Glass Powders Ternary Blended Concrete

**Moruf O. Yusuf [1,*], Khaled A. Alawi Al-Sodani, [1], Adeshina A. Adewumi [1], Muyideen Abdulkareem [2] and Ali H. Alateah [1]**

[1] Department of Civil Engineering, College of Engineering, University of Hafr Al Batin, P.O Box 1803, Hafr Al Batin 39524, Saudi Arabia

[2] Department of Civil Engineering & Quantity Surveying, Military Technological College, Muscat, Oman

* Correspondence: moruf@uhb.edu.sa

**Abstract**

Ternary blended concrete comprising flyash powder (FA), waste glass powder (WG) and ordinary Portland cement (OPC) were prepared such that the WG to total binder varied from 0-20% ($C_{80}FA_{20-x}G_x$: x = WG/(WG+FA+OPC)) at the interval of 0.05. The developed concrete was investigated for absorption, workability, 28-day compressive strength, product (binder) phases, bond characteristics, microstructural and elemental composition. The synergy of the proportion of WG and FA (5-15% and 10-10%) together with OPC (80%) reduced the workability, enhanced 28-day water absorption and produced moderately high compressive strength (47-48 MPa) that was about 15% lower than that recorded in pure OPC concrete (57.2 MPa). The binder with balanced proportion of FA and WG ($C_{80}FA_{10}G_{10}$) was found to be more amorphous with better microstructural stability than pure FA blended concrete ($C_{80}FA_{20}G_0$) due to pore-filling of the microcracks. Disappearance of hedenbergite phase ($CaFeSi_2O_6$) was noted in the developed ternary binder while more alumina in FA noticeably induced conversion of tobermorite (CSH to C-A-S-H in ternary binder. Besides, Si/Ca, Ca/Al and Si/Al ratios were higher in WG-FA balanced ternary binder ($C_{80}FA_{10}WG_{10}$) than when FA preponderated WG. Finally, using WG in synergy with FA could regulate absorption, consistency, amorphorsity and microstructure characteristics of FA-WG ternary binder.

**Keywords:** waste glass; admixtures; microstructures; construction materials; fly ash/ slags; high strength concrete

## 1. Introduction

Proliferation of greenhouse gases is another challenge that deserves attention to mitigate the challenges of global warming. Cement production industries contribute significantly to the proliferation of carbon dioxide in the calcination process, thereby releasing carbon dioxide as a greenhouse gas during the production of lime (CaO) required for the production of clinkers. Solid waste emanates from different sources such as agro, cement, and power generation industries. There has been indiscriminate solid waste deposition in the landfills, thereby constituting environmental pollutants that could affect public health negatively. There are many materials being used as supplementary materials in normal and high-performance concrete to achieve economy and environmental waste reduction in concrete production. These solid waste materials include silica fume (SF), flyash (FA), metakaolin (MK) and steel slag [1,2]. In recent times, stone dust, palm oil fuel ash (POFA) and waste glass (WG) have also been used towards achieving better strength and durability performances in concrete and mortar [3]. WG constitutes 7% of the world solid wastes [4] and 4.2% of 12.3 million of the solid wastes generated from the US in 2018 which could be categorized as total municipal solid wastes (MSW). The percentage of MSW being deposited in landfills

 doi:10.20944/preprints202508.1648.v1



amounted to 5.2% (7.6 million tons) (United State Environmental Protection Agency [5]). The annual recyclable glass in Australia is about 1 million tons [6] while the high content of impurity and the cost of transportation have made the recycling process inefficient. Glass Packaging Institute (GPI) reported that 3.1 million tons of recyclable was WG, while about 50% was reported was combusted glass. Effective preservation and efficient WG management processes and reduction in the annual ordinary Portland cement (OPC) consumption are very essential to reduce greenhouse gas and accumulated solid wastes in the environment.

Several researchers have studied contributions of WG to mechanical and durability properties of concrete. This paves way for the utilization of WG in the fragmented and powdered forms for fine aggregates and supplementary cementitious additives applications, respectively thereby reducing its accumulation in the landfill [7–10]. Several other types of glass such as cathode ray tube, solar panel and fluorescent lamps have equally been used to produce mortar and concrete. Replacing 20% ordinary Portland cement (OPC) with WG powder contributes to 90-day strength of concrete [11]. Tan et al. [9] also reported contribution of WG to density and rheology of concrete when used as fine aggregate, while Lu et al. [12] also linked extension of setting time, hydration process and flowability to the content of WG powder in concrete product. Rahma et al. [13] also asserted that there was a reduction in workability of glass blended concrete. Hollow glass microsphere waste has also been used as an anchor in polymer and lightweight mortar production [14].

Furthermore, the size and colour of the glass could control its chemical reactivity ([15,16]). Inclusion of WG reduces the early strength due to dilution effect that prevents hydration of alite during early days of strength development [6]. WG particles also contribute to microstructural refinement by retaining non-evaporable water within the capillary pore [17]. It also contributed to durability and transport properties such as electrical resistivity, pore discontinuity and tortuosity [18]. Kawalu et al. [19] used fragmented WG as fine aggregates in geopolymer and OPC mortar synthesis and found that that the strength of the binder was compromised with reduction in drying shrinkage. Althoey et al. ([20]) replaced fine aggregate with WG and fiber in natural fiber reinforced concrete to achieve eco-friendly concrete. Besides, Tan et al. [9] investigated the contribution of milled WG as sand in mortar and asserted that less than 30% of the additive could contribute to electrical resistivity and absorption, respectively. Furthermore, Yusuf et al. [21] also explored the performance of WG in synergy with silica fume (SF) and OPC as ternary blending for better understanding of its contribution to fresh, hardened and microstructural properties.

Fly ash powder (FA), on the other hand, is a by-product of combustion of coal combustion in power generating stations. It contributes to concrete workability and mechanical properties [22]. FA and mine tailing (MT) enhance the consistency of concrete as reported by Sunil et al. [23] without loss in flexural and split tensile strength. Moreover, Goksen et al. [24] studied the performance of WG and FA separately as partial supplementary cementitious material (SCM) for OPC with a view to mitigating the effect of alkaline silica reactivity (ASR) through reduction of concrete porosity, water absorption while increasing the binder strength. Jurczak et al. [25] reported that the replacement of WG blended concrete outperformed FA blended concrete in terms of strength and durability. FA and WG had also been used for glass production with significant increase in mechanical and surface properties [26,27]. Sunarsih et al. [28] also used FA towards better flexural and sorptivity properties in concrete.

Despite the plethora studies on the use of WG and FA as additives in concrete production, there has not been a detailed study on the microstructural characteristics and elemental composition of ternary blended products involving OPC, WG and FA. The developed concrete consists of OPC (80-100%) and WG+FA of 20% such that WG varied with FA in different ratios. Therefore, this study seeks to provide deeper understanding on the transport, strength and microstructural characteristics of the ternary blended concrete at different ages for structural application. Workability, water absorption, compressive strength and microstructural analyses using scanning electron microscope with energy dispersive spectroscopy (SEM/EDS), x-ray diffraction (XRD) and Fourier transform infrared (FTIR) spectroscopy techniques. Finally, it is expected that this study will contribute and

 doi:10.20944/preprints202508.1648.v1



promote the usage of WG+FA-based ternary concrete for sustainable infrastructural development in the region where these two materials contribute significantly to the environmental challenges -such as solid waste accumulation in landfills - which could pose a threat to the public health.

## 2. Materials and Methods

### *2.1. Binder Raw Materials*

Ordinary Portland cement (OPC) Type 1 cement was used in accordance with ASTM C 150 with apparent specific gravity of 3.15. Flyash (FA) is supplied by high-tech flyash (India) Private Limited with the oxides composition through X-ray fluorescence (XRF) as shown in Table 1 while X-ray diffractogram (XRD) is as shown in Figures 1 and 2.

**Table 1.** Oxides composition of raw materials.

| Oxide composition | Glass | Flyash | OPC |
|---|---|---|---|
| $SiO_2$ | 68.10 | 60.34 | 19.01 |
| $Al_2O_3$ | 0.90 | 28.11 | 4.68 |
| $Fe_2O_3$ | 0.60 | 3.71 | 3.20 |
| CaO | 14.50 | 1.34 | 66.89 |
| MgO | 1.80 | - | 0.81 |
| $Na_2O$ | 12.20 | 0.55 | 0.09 |
| $TiO_2$ | 0.00 | - | 0.22 |
| $K_2O$ | 0.80 | 1.00 | 1.17 |
| $P_2O_5$ | - | - | 0.08 |
| $SO_3$ | 0.40 | 0.80 | 3.66 |
| $MnO_2$ | - | - | 0.19 |
| $SiO_2 + Al_2O_3 + Fe_2O_3$ | 69.60 | 92.16 | 26.89 |
| SG | 2.48 | 2.38 | 3.14 |
| LOI (%) | 0.80 | 0.50 | 2.80 |
| Surface area ($m^2/g$) | 0.223 | 420 | 0.33 |

The waste glass powder (WG) was obtained from a dumpsite along Sinaya Road, Hafr Al-Batin, Kingdom of Saudi Arabia. The WG was placed and crushed in Los Angeles grinding machine and then later placed in oven at 105 $^oC$ for moisture removal. It was then ground with an electronic grinder with titanium blade and power rating of 1.4 kW, voltage and frequency of 220 V and 60 Hz, respectively.

**Table 2.** Coarse aggregates distribution.

| Coarse aggregate size (mm) | Percentage composition |
|---|---|
| 10 | 30 |
| 12 | 20 |
| 14 | 30 |
| 20 | 20 |

### *2.2. Aggregates*

Natural dune sand passing sieve 2.36 mm (No. 8) and complying with ASTM C 157/C 157M –08 was used as fine aggregates. Its fineness modulus was 3.3 while the relative density (water) was 2.71.

 doi:10.20944/preprints202508.1648.v1



Coarse aggregate was limestone minerals with sizes range of 10-20 mm and were used at saturated surface dry (SSD) condition (Table 2). The specific gravities of all materials are as shown in Table 3.

**Table 3.** Specific gravities of all the materials.

| Materials | Specific gravity values |
|---|---|
| Cement | 3.14 |
| Glass | 2.48 |
| Flyash | 2.38 |
| Sand | 2.71 |
| Coarse | 2.54 |

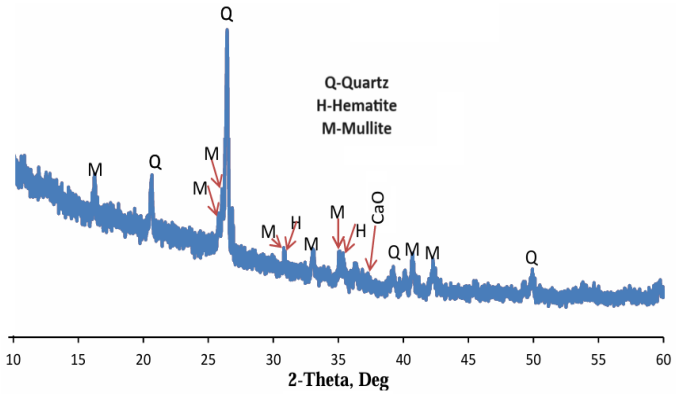


**Figure 1.** XRD Diffractogram of class F fly ash.

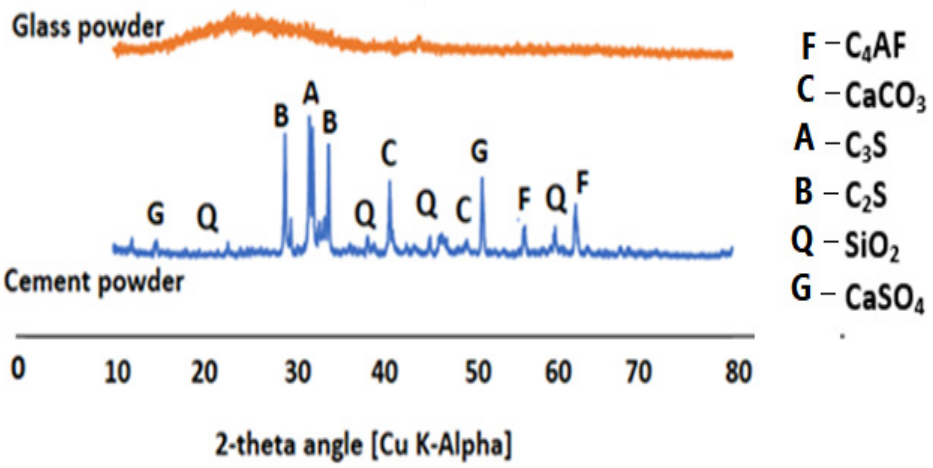


**Figure 2.** XRD diffractogram of glass waste and cement powder.

*2.3. Superplasticizer*

Glenum® superplasticizer of 0.5 wt.% of binders (cement, flyash and glass powder) was mixed with water to enhance the workability of the concrete. Glenum has been reported to have better performance and longer retention of slump than concrete mixtures containing melamine, naphthalene, and high range polycarboxylate water-reducing admixture.

 doi:10.20944/preprints202508.1648.v1



### *2.4. Sample Designation*

The mixture proportion of cement (OPC), waste glass (WG) and flyash (FA) in different proportions are presented in Table 4. The percentage of OPC was maintained at 80wt.% and 100% when both FA and WG were made to be 20%. The samples were categorized into tree, namely $C_{100}FA_0WG_0$ (OPC concrete), $C_{80}FA_{20}G_0$ (FA binary blended binder) and $C_{80}FA_{20-x}G_x$ (ternary blended concrete x = 5, 10, 15 and 20%).

### *2.5. Experimental Design*

#### 2.5.1. Workability

The workability of the concrete was tested using slump cone test in accordance with ASTM C 143. The difference in the height of concrete and the cone measured by meter rule is recorded as the stump value (in mm).

**Table 4.** Mix design for 1m3 ternary blended (OPC+FA+WG) concrete.

| Mixes | Flyash %FAs | Waste glass %WG | OPC % | w/b ratio | OPC Kg/m³ | Flyash Kg/m³ | WG Kg/m³ | Fine agg. Kg/m³ | Coarse Agg. Kg/m³ | water SSD | SP | Total density |
|---|---|---|---|---|---|---|---|---|---|---|---|---|
| **$C_{100}FA_0G_0$** | **0** | **0** | **100** | **0.4** | **350** | **0.0** | **0.0** | **753** | **1120** | **175** | **1.80** | **2400** |
| **$C_{80}FA_{20}G_0$** | **20** | **0** | **80** | **0.4** | **280** | **70.0** | **0.0** | **760** | **1120** | **168** | **1.80** | **2400** |
| $C_{80}FA_{15}G_5$ | 15 | 5 | 80 | 0.4 | 280 | 52.5 | 17.5 | 760 | 1120 | 168 | 1.80 | 2400 |
| **$C_{80}FA_{10}G_{10}$** | **10** | **10** | **80** | **0.4** | **280** | **35.0** | **35.0** | **760** | **1120** | **168** | **1.80** | **2400** |
| $C_{80}FA_5G_{15}$ | 5 | 15 | 80 | 0.4 | 280 | 17.5 | 52.5 | 760 | 1120 | 168 | 1.80 | 2400 |
| $C_{80}FA_0G_{20}$ | 0 | 20 | 80 | 0.4 | 280 | 0.0 | 70 | 760 | 1120 | 168 | 1.80 | 2400 |

#### 2.5.2. Water Absorption

The 28-day cubic concrete samples (100× 100 ×100 mm) of known mass was submerged in water for 24 hrs and thereafter mopped with towel to determine its saturated surface dry mass, $M_{ssd}$. The sample were then dried in oven (105 $^oC$, 24 hrs) to get, $M_{oven}$. Water absorption (at 28 days) is then calculated as shown in Equation (1):

$$\text{Water absorption} = \frac{M_{ssd} - M_{oven}}{M_{oven}} \text{x } 100 \quad (1)$$

#### 2.5.3. Compressive Strength Test

The compressive strengths at 7-, 14- and 28-d of the ternary blended concrete ($C_{80}FA_{20-x}G_x$) were determined using cubic sample sizes of 100 x 100 x 100 mm in accordance with BS EN 12390-3. The samples were crushed using universal testing machine at the loading rate of 0.9 kN/s. The average of three samples was recorded to obtain the desired strength at specific desired days.

#### 2.5.4. Characterization and Morphology of the Specimens

X-ray diffractometer (XRD), scanning electron microscopy/energy dispersive x-ray spectroscope (SEM + EDS) and Fourier transform spectroscopy (FTIR) were used to determine the compound (product) phases, microstructural morphology and bond characteristics of the product, respectively. The product phases were determined using XRD Bruker instrument model d2-Phaser with Cu Ka radiation (40 kV, 40 mA) by continuous scanning within 2-theta angle range of 4–80° at a scan speed of 2.5°/min. FTIR was determined by Perking Elmer 880 spectrometer while microstructural characterization of the 28-d cured paste was determined by JEOL SEM + EDS model 5800 LV at accelerating voltage of 20 kV.

 doi:10.20944/preprints202508.1648.v1



*2.6. Mix Design and Sample Preparations*

2.6.1. Mix Design

Concrete was produced by maintaining water to binder ratio and fine to total aggregates ratio at 0.4 (Table 4). The density of the concrete was approximately 2400 kg/m3. The total binders (OPC, FA and WG) was 350 kg/m3, with the combined (WG and FA) percentage of 20wt% (70 kg) while OPC was kept at 80 wt.% (280 kg) for the ternary blended concrete while FA+WG = 0 and OPC=100% for the control sample. The waste glass (WG/(FA+WG+OPC)) in ternary blended samples varied as 0, 5%, 10%, 15% and 20% while FA varied as 20, 15, 10, 5 and 0 wt.%, respectively.

2.6.2. Sample Preparation

The sample was prepared according to the mix design presented in Table 4 by first putting 75% of total water mixed with superplasticizers in the mixer. OPC, WG and FA powders were then put into the rotary mixer and then mixed for 3 mins. Fine and coarse aggregates were then added and further mixed for additional 4 mins, while the remaining water (25%) was subsequently added. The total mixture was thoroughly mixed homogenously for additional 4 mins before being emptied into the oil smeared mould of 100×100×100 mm after being properly compacted into three layers. The surface of the sample in the mould was smoothened by hand troweled and then covered with polythene sheet to prevent moisture loss. The sample were demoulded and kept inside curing tank at room temperature in the laboratory until it was ready for testing after allowing it to drain for at least 6 hrs. Afterwards, the slump was determined by using cone test (ASTM C143) using oil smeared mould 100×200×300 mm.

## 3. Discussion of Results

*3.1. Workability of Glass-Flyash Ternary Blended Concrete*

Figure 3 shows that flyash (FA) blended concrete ($C_{80}FA_{20}G_0$) has the highest consistency of all the mixtures due to its particle spherical nature. This also corroborates the finding of Gökşen et al. (2023) where FA was reported to improve the consistency of a blended concrete excessively due to the lubrication on aggregate particles. The flowability of $C_{80}FA_{20}G_0$ was 37.1% more than that obtained from OPC concrete ($C_{100}FA_0G_0$). By incorporating the combined WG and FA in varying proportion of 5-10% in partial replacement for OPC ($C_{80}FA_{15}G_5$ and $C_{80}FA_{10}G_{10}$), the workability reduced by 21% and 8.1%, respectively with reference to FA blended sample ($C_{80}FA_{20}G_0$). In comparison with OPC concrete ($C_{100}FA_0G_0$), the consistency of $C_{80}FA_{15}G_5$ and $C_{80}FA_0G_{20}$ reduced by 8.1% and 27.4%. The Use of 5% WG and 15% FA ($C_{80}FA_{15}G_5$) could attain slump value of 75 mm which is enough for fresh concrete for many structural applications as Figure 3 shows the workability of pure OPC cement concrete to be 62 mm ($C_{100}FA_0G_0$).

Furthermore, the workability of $C_{80}FA_{20}G_0$ reduced by 11.8%, 21.2%, 32.9%, and 47.10%, respectively upon adding 5, 10, 15 and 20% of WG as x values in $C_{80}FA_{20-x}G_x$, respectively. The synergy of both WG and FA impeded the lubricating effect of FA particles interactions with the aggregates thereby increasing the energy required to overcome interparticle friction. The reduction in consistency was due to irregular shapes of WG thereby enhancing the interparticle friction that hinders the flow. Thus, impact WG on FA blended concrete on workability performance of the ternary blended concrete could vary depending on the WG/FA ratios. This provides the opportunity for economic use of waste materials to enhance and modify the fresh properties of OPC based concrete towards achieving a desired concrete workability.

 doi:10.20944/preprints202508.1648.v1



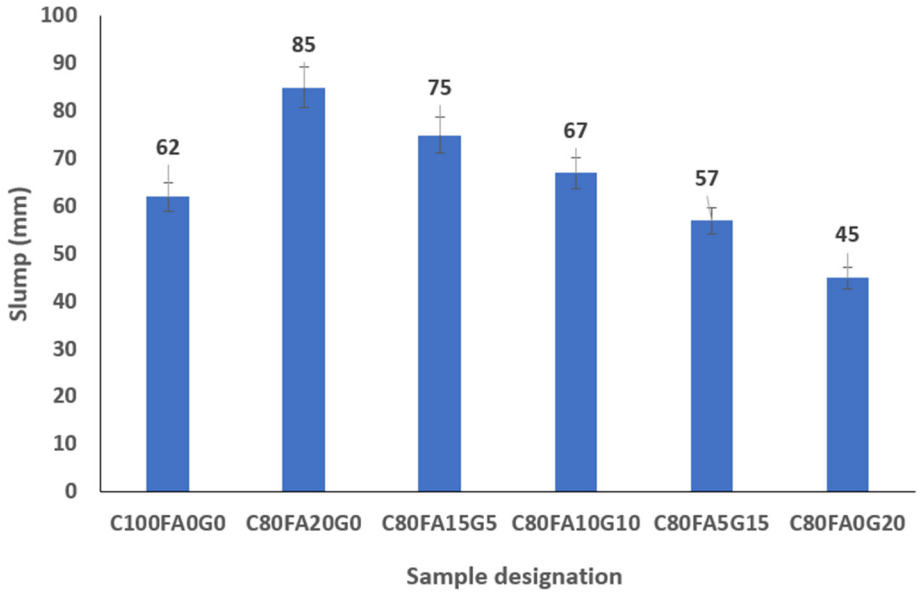


**Figure 3.** Workability of fly ash-waste glass ternary blended concrete.

*3.2. Absorption of Flyash-Waste Glass Ternary Blended Concrete*

Figure 4 shows that incorporation of 20% of WG+FA in varying quantities (WG/(WG+FA) = 0, 5%,10%, 15% and 20%) into the 28-d ternary blended concrete ($C_{80}FA_{20-x}G_x$) linearly increase the water intake capacity. The presence of only FA just increased the absorption of OPC concrete by 4%. Similarly, Golewski [29] reported 6% increase in absorption of OPC concrete upon incorporating 20% FA.

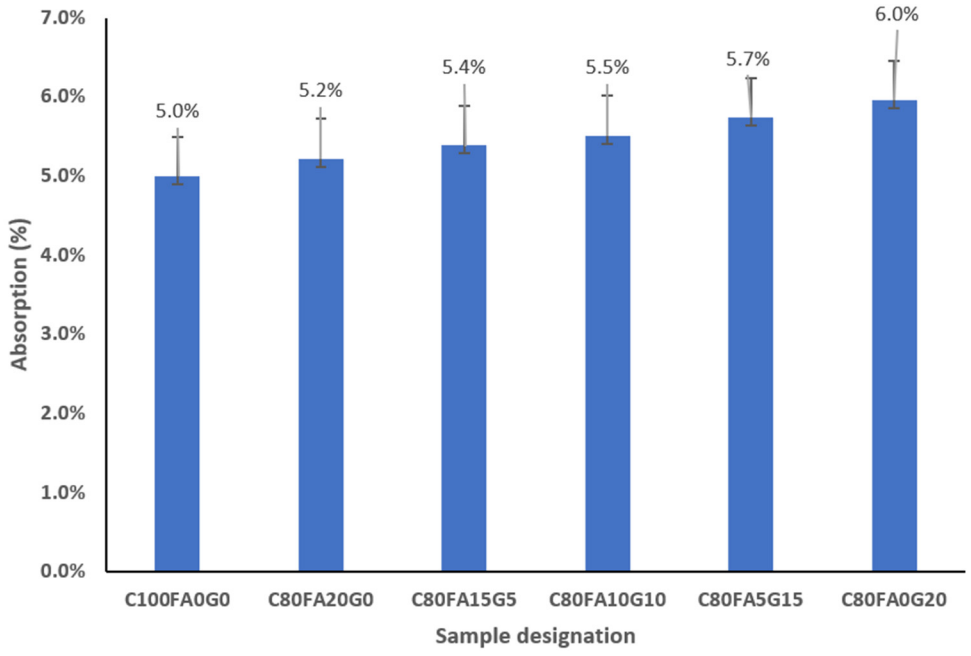


**Figure 4.** Water absorption in flyash-glass ternary blended concrete.

This implies that absorption of ternary concrete increases with preponderance of WG over FA due to its irregular particle shape and more capillary action that favors water permeability in the interfacial transition zone within the aggregates and paste in the concrete matrix. Besides, higher WG/FA ratio could be responsible for the widening of capillary pores thereby decreasing the tortuosity of the binder matrix. Figure 4 shows that the percentages of water intakes obtained in $C_{80}FA_{20}G_0$, $C_{80}FA_{15}G_5$, $C80FA_{10}G_{10}$, $C_{80}FA_5G_{15}$ and $C_{80}FA_0G_{20}$ increased by 4, 8, 10, 14 and 20%,

 doi:10.20944/preprints202508.1648.v1



respectively in comparison with OPC concrete (C100FA0G0). This is also in agreement with what was previously reported (Guo et al., 2020). This indicates that the synergy of WG and FA in concrete production - in excess of WG - enhances the porosity of concrete thereby making the use of these additives relevant in the production of porous concrete.

*3.3. Compressive Strength of Glass-Flyash Ternary Blended Concrete*

The compressive strength of ternary blended concrete ($C_{80}FA_{20-x}WG_x$) shown in Figure 5 indicates that 3-d early strength of $C_{80}FA_{20-x}G_x$ decreases with WF/FA ratios. The lowest 3-d early strength $C_{80}FA_0G_{20}$ and $C_{80}FA_{20}G_0$ were 25 MPa and 29.3 MPa, respectively while it was 32 MPa in OPC concrete ($C_{100}FA_0G_0$). Furthermore, the 3-day strengths recorded in $C_{80}FA_{20}G_0$, $C_{80}FA_{15}G_5$, $C_{80}FA_{10}G_{10}$, $C_{80}FA_5G_{15}$ and $C_{80}FA_0G_{20}$ reduced by 8.43, 14.71, 17.03, 25, and 21.88%, respectively in comparison with OPC concrete. The reason for the decrease could be adduced to early day dilution effect on strength development as induced by FA and WG. Moreover, the compressive strength was noticeably decreasing with increase in WG/FA ratio with the lowest value recorded in WG blended sample ($C_{80}FA_0G_{20}$). It can be said that adding FA (10-15%) in synergy with WG enhanced the strength of the ternary blended concrete better than what is obtainable in binary blended concrete of OPC-FA or OPC-WG-based independently. Thus, higher WG/FA ratios had more debilitating impacts than the lower WG?FA ratio on the achievable strength in the synthesis ternary blended concrete.

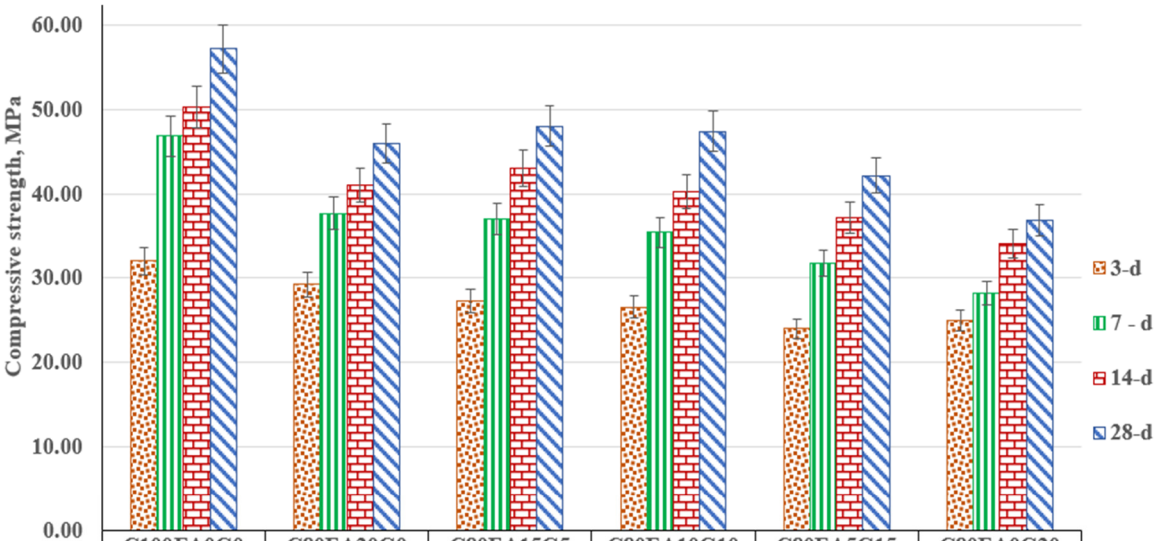


| | C100FA0G0 | C80FA20G0 | C80FA15G5 | C80FA10G10 | C80FA5G15 | C80FA0G20 |
|---|---|---|---|---|---|---|
| 3-d | 32.00 | 29.30 | 27.29 | 26.55 | 24.00 | 25.00 |
| 7 - d | 46.80 | 37.68 | 37.05 | 35.40 | 31.80 | 28.20 |
| 14-d | 50.30 | 41.00 | 43.00 | 40.30 | 37.20 | 34.10 |
| 28-d | 57.20 | 46.00 | 48.00 | 47.40 | 42.15 | 36.90 |

**Figure 5.** Compressive strength of glass-fly ash ternary blended concrete.

A similar trend was also observed at 7-14 day of strength development when the strength recorded in OPC concrete ($C_{100}FA_0G_0$) is compared to those recorded in blended samples. For instance, $C_{80}FA_{20}G_0$ $C_{80}FA_{15}G_5$ $C_{80}FA_{10}G_{10}$, $C_{80}FA_5G_{15}$ and $C_{80}FA_0G_{20}$ are lower than the result obtained in OPC concrete by educed by 8.9, 16.1, 13.8, 17.0 and 21%, respectively. The optimal strength of 46-48 MPa could be achieved in ternary blending structural concrete ($C_{80}FA_{20-x}WG_x$) with adequate mixing, curing and compaction when x varied between 0, 5, and 10% while WG/FA ratios were within 0.33-1.0. Figure 6 depicts the relationship between the experimental and predicted strength models in WG-FA ternary blended concrete with high regression coefficient of 0.86 ($R^2$ = 0.856) as shown in Equation (2). The parameters used in the model include age (3,7,14, and 28 days), OPC (80-100%), WG (0-20%) and FA (0-20%) together with their possible combinations.

 doi:10.20944/preprints202508.1648.v1



$$f'_c = 19.95Age^{0.2387} + 3.21 \times 10^{-217}(OPC)^{85.52} + 2.883 \times 10^{-6}(FA \times WG)^{1.9277} + 9.63 \times 10^{-50}(FA \times OPC \times WG)^{9.0085} \quad (2)$$

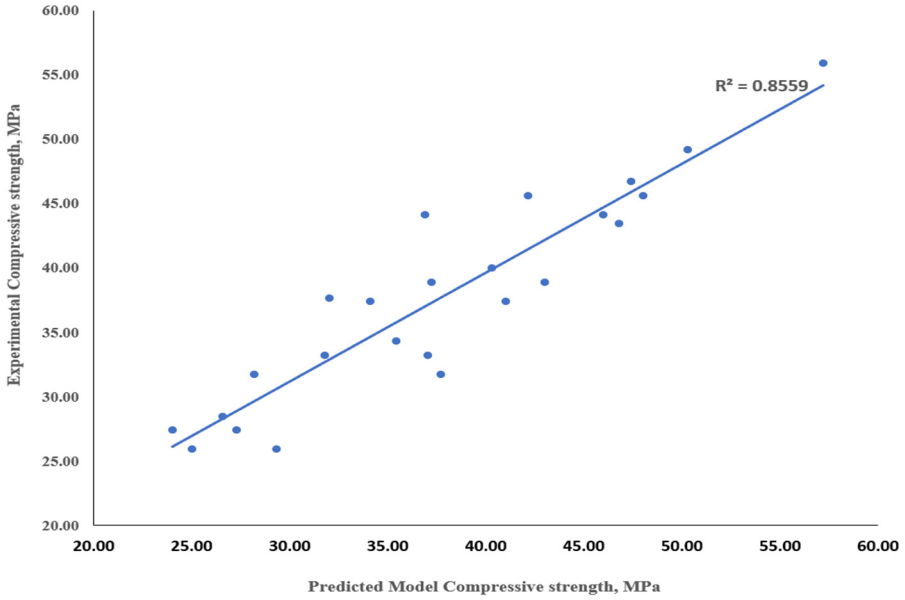


**Figure 6.** Correlation of experimental and predicted strengths in glass waste/fly ash blended concrete.

*3.4. Microstructural Characteristics and Elemental Analyses of the Products*

Figure 7a,c shows the morphology of FA-OPC binary blended paste ($C_{80}FA_{20}G_0$) at 28 days while Figure 7b,c depicts the ternary blended sample comprising FA and WG ($C_{80}FA_{10}G_{10}$) at the same age. The microstructure of pure fly ash blended concrete ($C_{80}FA_{20}G_0$) is characterized by discontinuity due to micropores and microcracks while that with WG a better microstructural stability (Figure 7a,c). This shows that WG provided pore filling or packing effect in the presence of FA within the OPC capillary pore as shown in $C_{80}FA_{10}G_{10}$ (Figure 7b,c). In the morphology presented in Figure 7c, EDS reveals that Ca/Si in reduced from 3.82 ($C_{80}FA_{20}G_0$) to 3.36 in $C_{80}FA_{10}G_{10}$ due to the presence of high Si relative to Ca in WG compared to FA and OPC as noted in the XRF results (Table 1, Table 5 and Figure 7c). This suggests that silicate re-organization could be better achieved in WG-FA-OPC ternary system ($C_{80}FA_{10}G_{10}$) binary systems with the absence of either of WG and FA ($C_{80}FA_0G_{20}$ and $C_{80}FA_{20}G_0$. Furthermore, it is also noticeable that the presence of more Al in FA compared to WG and OPC has a debilitating effect on the compressive strength and microstructural stability up to 28-day strength development. From Figure 7c increase in Si/Al from 3.0 ($C_{80}FA_{20}G_0$) to 3.69 ($C_{80}FA_{10}G_{10}$), further, the presence of low Si/Al ratio with the C-S-H formation has been reported to be responsible for the formation of calcium aluminosilicate hydrate (C-A-S-H). Table 5 also points to more Ca/Al (12.5) in ternary blended ($C_{80}FA_{10}G_{10}$) compared to FA based binary concrete ($C_{80}FA_{20}G_0$) that has Ca/Al ratio of 11.46.

This is an indication of better structural stability of the ternary synthesis in comparison with the binary due to the possibility of formation of amorphous C-A-S-H together with C-S-H. Figure 8 points to this fact due to the absence of tobermorite that is conspicuously visible in OPC binder but absent in $C_{80}FA_{20}G_0$ and $C_{80}FA_{10}G_{10}$.

 doi:10.20944/preprints202508.1648.v1



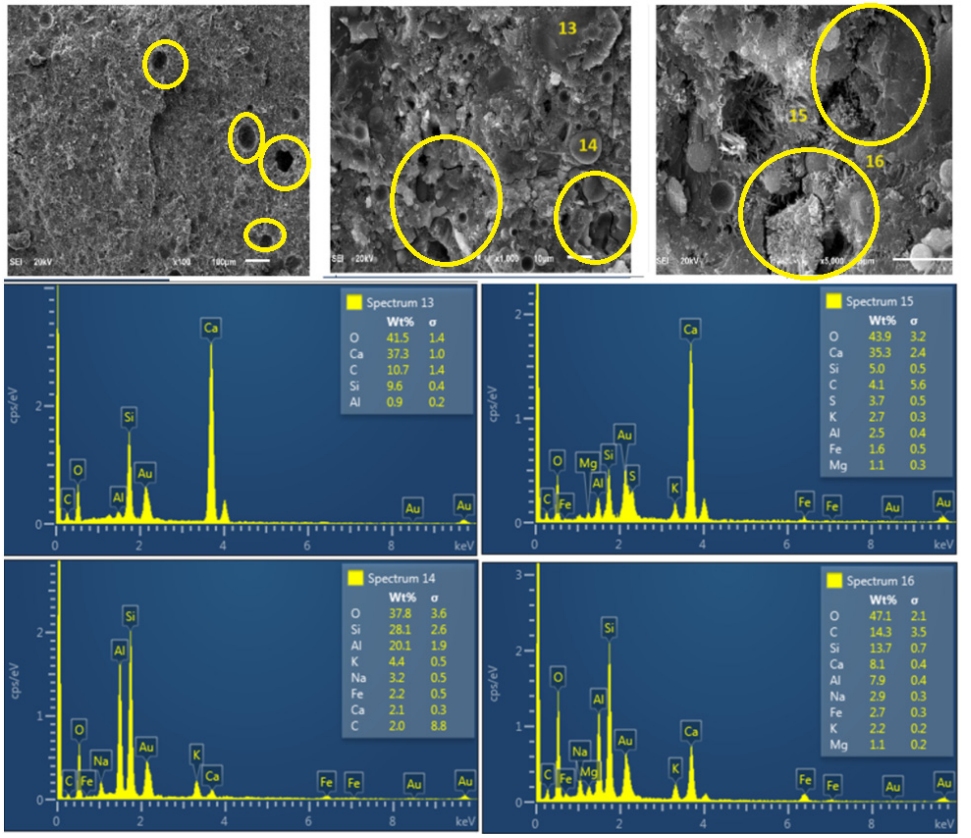


(**a**)

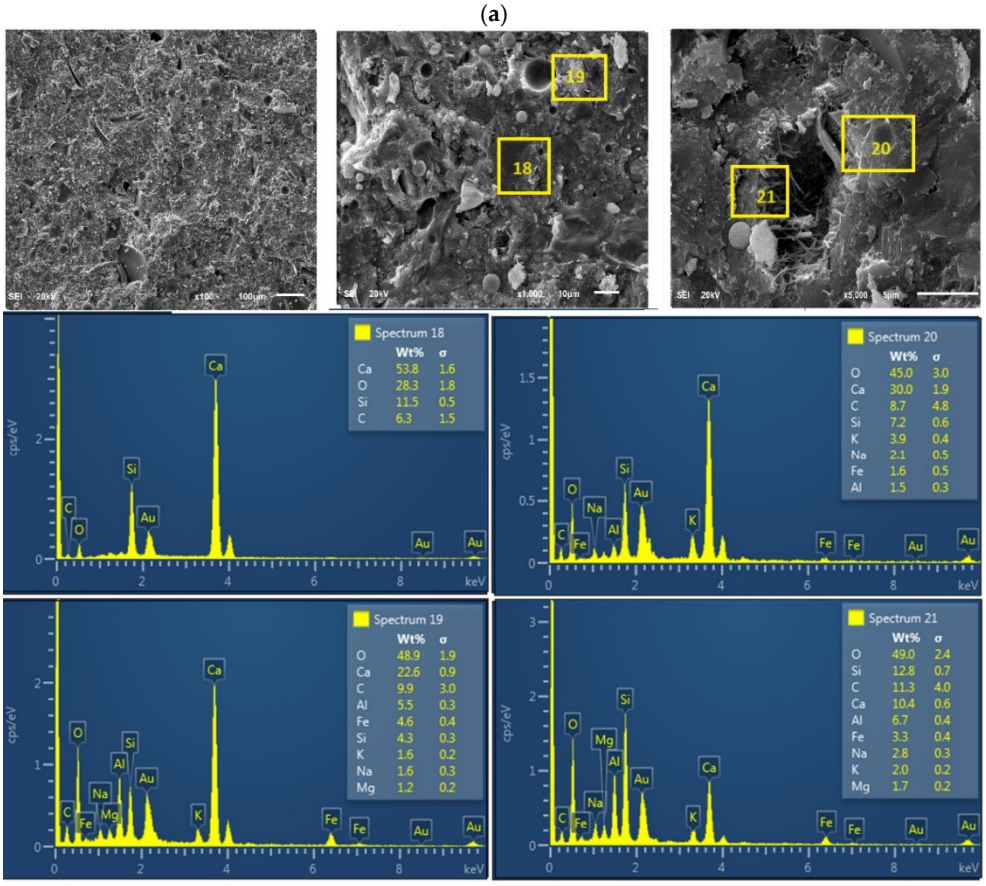


(**b**)

 doi:10.20944/preprints202508.1648.v1



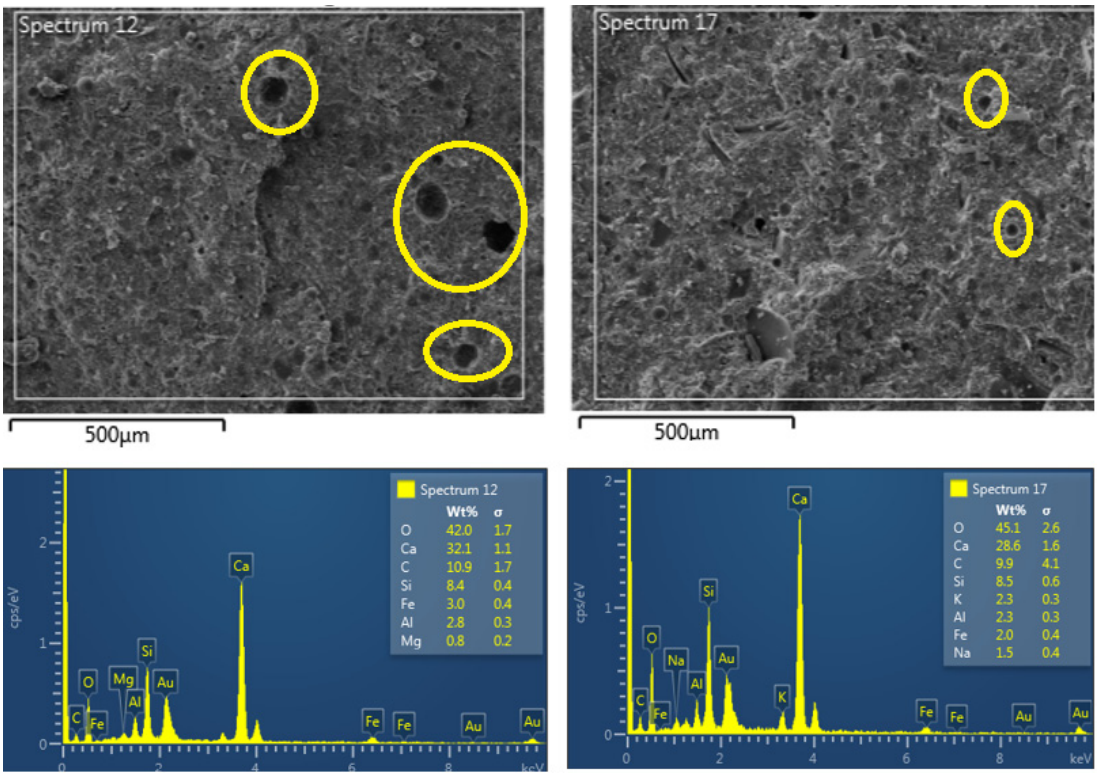


(**c**)

**Figure 7.** a: Morphology of 28-day flyash bended (C80FA20G0) paste. b: Morphology of ternary blended waste glass flyash (C80FA10G10) paste. 7c: Morphology and EDS of the binary (C80FA20G0 - left) and ternary (C80FA10G10 -right) paste.

**Table 5.** EDS Elemental composition of the binders.

| | Flyash-OPC Paste | Flyash-Glass-OPC Paste |
|---|---|---|
| Elemental ratio | $C_{80}FA_{20}G_0$ | $C_{80}FA_{10}G_{10}$ |
| Ca/Si | 3.82 | 3.39 |
| Ca/Al | 11.46 | 12.52 |
| Si/Al | 3.00 | 3.69 |

*3.5. X-Ray Diffraction of the Flyash-Glass Ternary Blended Binder*

Figure 8 shows the prominent features common to all the three binders which include ettringite ($Ca_6Al_2(SO_4)_3(OH)_{12}\cdot 26H_2O$), calcium silicate hydrate (C-S-H) ($Ca_5Si_6O_{16}(OH)_2.4H_2O$), calcite ($CaCO_3$), merwinite ($Ca_3Mg(SiO_4)_3$), quartz ($SiO_2$) and portlandite ($Ca(OH)_2$).

 doi:10.20944/preprints202508.1648.v1



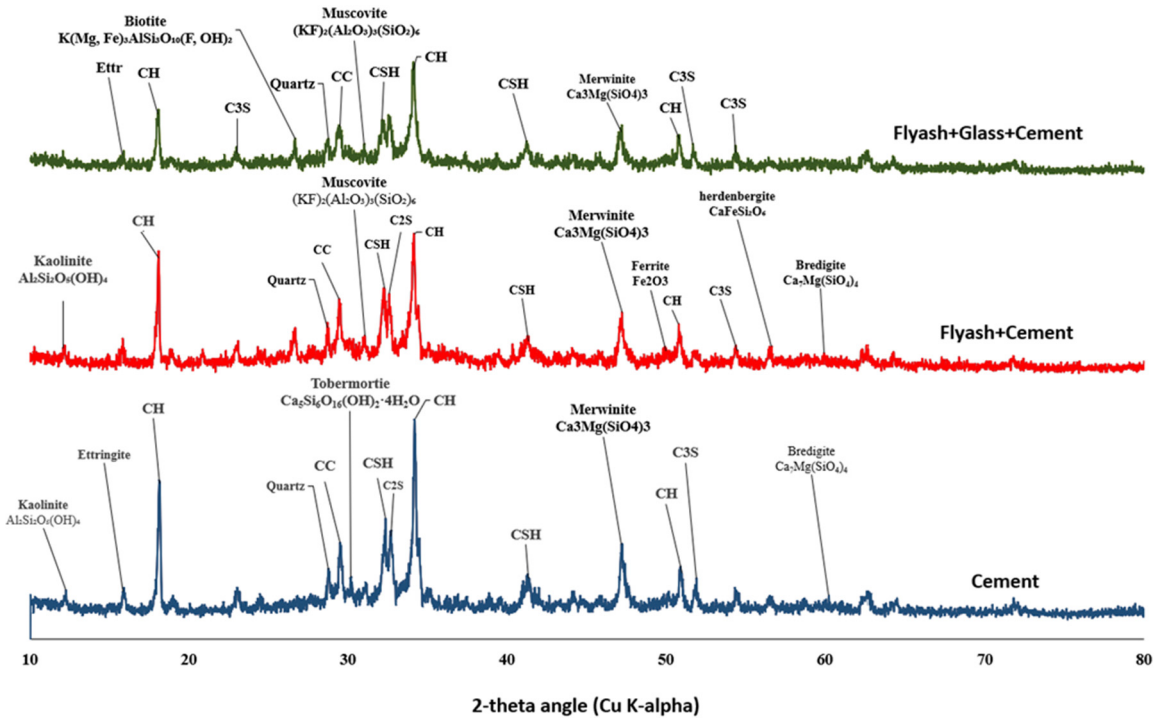


**Figure 8.** XRD diffractogram of flyash-glass blended binder (C80FA10C10 - top), Flyash blended binder (C80FA20C10 - middle) and OPC cement binder (C100FA0C0 - bottom).

Synergy of WG with FA improved the amorphousity of the product ($C_{80}FA_{10}G_{10}$) due to disappearance of bredigite ($CaMg(SiO_4)_4$, hedenbergite ($CaFeSi_2O_6$) tobermorite, and ferrites in ternary blended binder ($C_{80}FA_{10}G_{10}$) but present in FA-blended binder ($C_{80}FA_{20}G_0$) diffractogram. However, both FA-blended and ternary blended binders ($C_{80}FA_{10}G_{10}$ and $C_{80}FA_{20}G_0$) have muscovite ($(KF)_2(Al_2O_3)_3(SiO_2)_4$) and biotite ($K(Mg,Fe)_3AlSi_3O_{10}(F,OH)_2$) as the main crystalline phases while these were notably absent in OPC system ($C_{100}FA_0G_0$). Poorly crystalline phase of tobermorite (C-S-H) is also found in OPC system but notably disappeared and suspectedly replaced by amorphous C-A-S-H due to lower Si/Al in FA-composed systems ($C_{80}FA_{10}G_{10}$ and $C_{80}FA_{20}G_0$) as shown in Figure 8.

*3.6. Bond Characteristics of Binary (FAP-OPC) and Ternary Blended (WGP/FAP/OPC) Binders*

Figure 9 indicates that the presence of WG in synergy with FA and OPC (WG+FA+OPC - $C_{80}FA_{10}G_{10}$) has different bond characteristics with FA-based binary binder (FA+OPC - $C_{80}FA_{20}G_0$) and pure OPC binder ($C_{100}FA_0G_0$). For instance, the bending vibration of Si-O-Si(Al) was noted at wavenumber 511, 451, 457 $cm^{-1}$ with the highest vibration in OPC system and the lowest in FA-based binary system. Gosh et al. [30,31] and (Yusuf, 2023) assigned the bending vibration of tetrahedral silicate (Si-O-Si(Al)) at 400-520 $cm^{-1}$ due to the presence of C-S-H, tobermorite and unreacted alite/belite in OPC binder. This indicates that there was more Al-O stretching vibration in $C_{80}FA_{20}G_0$ than in $C_{80}FA_{10}G_{10}$ due to the presence of Al-O-Si bond vibration. This indicates that the formation of (C-A-S-H) product is possibly in FA-based binder. The presence of FA together with WG is the main reason while Al-O-Si vibration in both systems are very close in values (451 and 457 $cm^{-1}$). This also explains the reason why FA-OPC systems ($C_{80}FA_{20}WG_0$) is noticeably less amorphous compared to WG-FA-OPC system ($C_{80}FA_{10}G_{10}$) as indicated in Figure 8 (XRD results).

Furthermore, the asymmetric stretching of Si-O-Al vibration is 870-874 $cm^{-1}$ with the highest vibration (874 $cm^{-1}$) was observed in the more heterogenous ternary blended paste ($C_{80}FA_{10}G_{10}$) compared to less heterogenous FA-OPC ($C_{80}FA_{20}G_0$) system (872 $cm^{-1}$) with the lowest value recorded in OPC system ($C_{100}FA_0G_0$) (870 $cm^{-1}$).

There is also an asymmetric Si-O-Si bond vibrations within 900-1200 $cm^{-1}$ [31] with specifically values of 991 $cm^{-1}$ in OPC paste, 980 $cm^{-1}$ in OPC-FA binders and 963 $cm^{-1}$ in ternary binder. This is

 doi:10.20944/preprints202508.1648.v1



due to high Si-O-Si bonds defining tobermorite in the calcium silicate hydrate with the consequent increase in the compressive strength as presented in Figure 5. The reduction in the ternary and ternary system could be replacement of tobermorite with C-(A)-S-H.

Moreover, hydrogen bonding (H-OH) vibrations (2918 and 2922 $cm^{-1}$) defined the blended binder ($C_{80}FA_{20}G_0$ and $C_{80}FA_{10}G_{10}$) but this band is absent in OPC system ($C_{100}FA_0G_0$). This could be due to effect of dilution of the nucleation site that induces the formation of $Al(OH)_3$ during the hydration process at the expense of formation of portlandite in blended system (ternary or binary). Adsorbed water vibration is less in $C_{80}FA_{10}G_{10}$ (1645 $cm^{-1}$) compared to $C_{80}FA_{20}G_0$ (1647 $cm^{-1}$). This bands point to the vibration of adsorbed water molecules within the capillary pores with the highest value in OPC system compared to other systems. Carbonation process that led to the formation of calcite (O-C-O bonds) is noted at the bands 1423 and 1425 $cm^{-1}$ [31]. The presence of calcite in the XRD shown in Figure 8 indicates that the carbonation process happens in the three systems due to the presence of portlandite or hydroxyl attached compound interaction with carbondioxide to form calcium carbonate or calcite. All the three samples were susceptible to environmental carbonation (O-C-O in $CO_3^{2-}$) at different wavenumbers ranging from 2345-2350 $cm^{-1}$. The least value was recorded in ternary blended sample ($C_{80}FA_{10}G_{10}$) while the highest was observed FA-OPC system ($C_{100}FA_0G_{10}$) due to difference in their structural parking density.

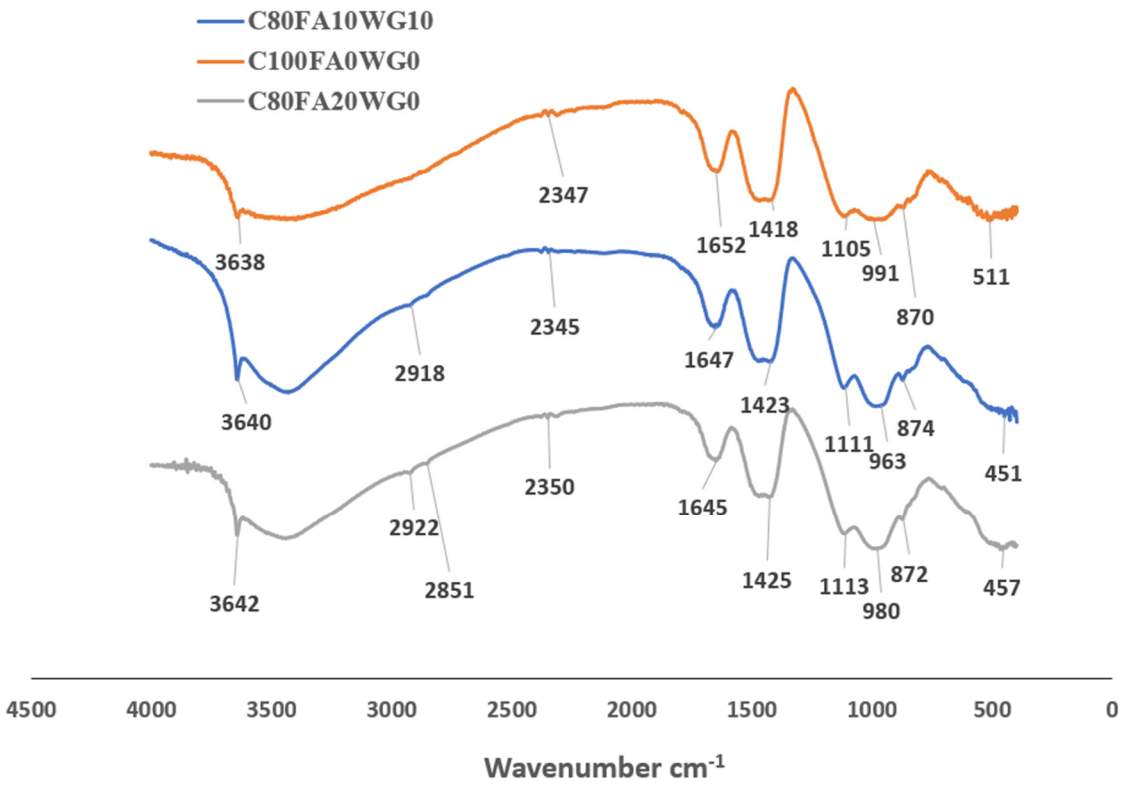


**Figure 9.** FTIR spectra of hydrated cement ($C_{100}FA_0G_0$-top), glass-flyash-cement ($C_{80}F_{10}G_{10}$-middle) and flyash blended cement ($C_{80}FA_{20}G_0$-bottom) paste.

 doi:10.20944/preprints202508.1648.v1



## 4. Conclusions

This study investigates the performance of ternary blended concrete made from ordinary Portland cement (OPC), flyash (FA) and waste glass (WG) in terms consistency, absorption, compressive strength, product phases, bonds and microstructural characteristics such that WG/(WG+FA+OPC) varied from 0 to 20% by the weight of the total binders. The following are the main conclusions:

- The impact WG on FA blended concrete on workability performance of the ternary blended concrete could vary depending on the WG/FA ratios.
- The synergy of WG and FA in concrete production when WG preponderates FA enhanced the porosity and absorption of ternary blended concrete thereby making the use of these additives relevant in the production of porous concrete. However, this had negative impact on the compressive strength of the binder.
- Structural concrete of 28-day strength of 46-48 MPa could be obtained in ternary blended concrete if FA preponderates WG at the minimum percentage composition of 10-15% and 5-10%, respectively as the combined effect of WG and FA had positive correlation on the achievable strength coefficient.
- Ternary blended concrete of balanced WG and FG proportion ($C_{80}FA_{10}WG_{10}$) had better morphological characteristics due to elimination of micro-pores, and better microstructural density compared to binary blended concrete without WG ($C_{80}FA_{20}WG_{0}$).
- Energy dispersive spectroscopy (EDS) indicates that silicate reorganization could be better in ternary blended concrete than the binary blended due to more Si/Al, Si/Ca and Ca/Al ratios in $C_{80}FA_{10}WG_{10}$ in comparison with FA blended concrete ($C_{80}FA_{20}G_{0}$). Therefore, the use of ternary blending concrete promotes reduction of environmental solid wastes.
- Fourier transform infrared spectroscopy (FTIR) reveals that the compressive strength is directly related to Si-O-Si asymmetric stretching vibrations. Bending of Si-O-Al band (511 $cm^{-1}$) and adsorbed water (H-O-H) (1652 $cm^{-1}$) vibrations within the capillary pores is higher in OPC binder system ($C_{100}FA_{0}G_{0}$) compared to that of binary (FA-OPC, $C_{80}FA_{20}G_{0}$) and ternary blended (FA-WG-OPC, $C_{80}FA_{10}G_{10}$) binder systems.
- X-ray diffractogram (XRD) indicates the amorphous nature of the product achieve through ternary blending depends on WG/FA ratio. Incorporation of WG with FA-OPC blended binder led to the disappearance of hedenbergite phase ($CaFeSi_2O_6$) in $C_{80}FA_{10}G_{10}$ (ternary blended system) despite their presence in $C_{80}FA_{20}G_{0}$. There was also disappearance of poorly crystalline tobermorite (C-S-H) phase present in OPC binder in ternary binder system due to the formation of more amorphous product.
- Finally, the use of these additives (WG and FA) promotes valorization of solid waste thereby leading to the reduction of volume of landfills. It also promotes clean environment and economic concrete production in the areas where these wastes pose environmental challenges.

**Funding:** This research is funded by the Deanship of Research and Innovation at University of Hafr Al Batin through the project number 0170-1446-S.

**Data availability statement:** The raw data needed for results reproduction are cited in the manuscript.

**Acknowledgements:** The continuous support of the University of Hafr Al Batin is highly appreciated.

**Competing interest:** The Author declares that there is no competing interest

### References

1. A.K. Parande, "Role of ingredients for high strength and high-performance concrete – a review," *Advances in Concrete Construction*, vol. 1, no. 2, pp. 151–162, Jun. 2013, Accessed: Apr. 08, 2025. [Online]. Available: https://doi.org/10.12989/acc.2013.1.2.151

 doi:10.20944/preprints202508.1648.v1




2. H. S. Chore and M. P. Joshi, "Strength evaluation of concrete with fly ash and GGBFS as cement replacing materials," *Advances in concrete construction*, vol. 3, no. 3, pp. 223–236, Sep. 2015, doi: 10.12989/acc.2015.3.3.223.
3. Imrose B. Muhit, Muhammad T. Raihan, and MD. Nuruzzaman, "Determination of mortar strength using stone dust as a partially replaced material for cement and sand. ," *Advances in Concrete Construction An Int'l Journal* , vol. 2, no. 4, pp. 249–559, 2014.
4. Q. Li, H. Qiao, A. Li, and G. Li, "Performance of waste glass powder as a pozzolanic material in blended cement mortar," *Constr Build Mater*, vol. 324, no. February, p. 126531, 2022, doi: 10.1016/j.conbuildmat.2022.126531.
5. 1991; EPA, "Environmental Protection Agency."
6. N. Tamanna and R. Tuladhar, "Sustainable Use of Recycled Glass Powder as Cement Replacement in Concrete," *The Open Waste Management Journal*, vol. 13, no. 1, pp. 1–13, 2020, doi: 10.2174/1874347102013010001.
7. J. Cao, J. Lu, L. Jiang, and Z. Wang, "Sinterability , microstructure and compressive strength of porous glass- ceramics from metallurgical silicon slag and waste glass," *Ceram Int*, vol. 42, no. 8, pp. 10079–10084, 2016, doi: 10.1016/j.ceramint.2016.03.113.
8. B. Singh and R. Jain, "Use of waste glass in concrete : A review," *J Pharmacogn Phytochem*, vol. 5, pp. 96–99, 2018.
9. K. H. Tan and H. Du, "Use of waste glass as sand in mortar: Part i - Fresh, mechanical and durability properties," *Cem Concr Compos*, vol. 35, no. 1, pp. 109–117, 2013, doi: 10.1016/j.cemconcomp.2012.08.028.
10. H. Zhao, C. S. Poon, and T. C. Ling, "Utilizing recycled cathode ray tube funnel glass sand as river sand replacement in the high-density concrete," *J Clean Prod*, vol. 51, pp. 184–190, 2013, doi: 10.1016/j.jclepro.2013.01.025.
11. G. M. S. Islam, M. H. Rahman, and N. Kazi, "Waste glass powder as partial replacement of cement for sustainable concrete practice," *International Journal of Sustainable Built Environment*, vol. 6, no. 1, pp. 37–44, 2017, doi: 10.1016/j.ijsbe.2016.10.005.
12. J. X. Lu and C. S. Poon, "Use of waste glass in alkali activated cement mortar," *Constr Build Mater*, vol. 160, pp. 399–407, 2018, doi: 10.1016/j.conbuildmat.2017.11.080.
13. A. Rahma, N. El Naber, and S. I. Ismail, "strength and the workability of concrete Effect of glass powder on the compression strength and the workability of concrete," *Cogent Eng*, vol. 7, no. 1, 2017, doi: 10.1080/23311916.2017.1373415.
14. V. A. Perfilov and V. S. S. D. V. Oreshkin, "Environmentally Safe Mortar and Grouting Solutions with Hollow Glass Microspheres," in *International Conference on Industrial Engineering*, Procedia Engineering 150: ICIE 2016, 2016, pp. 1479–1484.
15. M. Mirzahosseini and K. A. Riding, "Effect of curing temperature and glass type on the pozzolanic reactivity of glass powder," *Cem Concr Res*, vol. 58, pp. 103–111, 2014, doi: 10.1016/j.cemconres.2014.01.015.
16. M. Mirzahosseini and K. A. Riding, "Influence of different particle sizes on reactivity of finely ground glass as supplementary cementitious material (SCM)," *Cem Concr Compos*, vol. 56, pp. 95–105, 2015, doi: 10.1016/j.cemconcomp.2014.10.004.
17. M. Kamali and A. Ghahremaninezhad, "An investigation into the hydration and microstructure of cement pastes modified with glass powders," *Constr Build Mater*, vol. 112, pp. 915–924, 2016, doi: 10.1016/j.conbuildmat.2016.02.085.
18. M. Carsana, M. Frassoni, and L. Bertolini, "Comparison of ground waste glass with other supplementary cementitious materials," *Cem Concr Compos*, vol. 45, pp. 39–45, 2014, doi: 10.1016/j.cemconcomp.2013.09.005.
19. N. Kawalu, A. Naghizadeh, and J. Mahachi, "The effect of glass waste as an aggregate on the compressive strength and durability of fly ash-based geopolymer mortar," *MATEC Web of Conferences*, vol. 361, p. 05007, 2022, doi: 10.1051/matecconf/202236105007.
20. F. Althoey, O. Zaid, A. Majdi, F. Alsharari, S. Alsulamy, and M. M. Arbili, "Effect of fly ash and waste glass powder as a fractional substitute on the performance of natural fibers reinforced concrete," *Ain Shams Engineering Journal*, vol. 14, no. 12, Dec. 2023, doi: 10.1016/j.asej.2023.102247.

 doi:10.20944/preprints202508.1648.v1




21. M. O. Yusuf et al., "Performances of the Synergy of Silica Fume and Waste Glass Powder in Ternary Blended Concrete," *Applied Sciences*, vol. 12, no. 13, 6637, pp. 1–16, 2022.
22. B. , Clazer, C. , Garber, C. , Roose, P. , Syrett, and C. Youssef, "Fly ash in Concrete," 2011.
23. Sunil B.M, Manjunatha L.S., Lolitha Ravi, and Subhash C.Yaragal, "Potential use of mine tailings and fly ash in concrete.," *Advances in Concrete Construction, An Int'l Journal* , vol. 3, no. 1, 2015.
24. Y. Gökşen et al., "Synergistic effect of waste glass powder and fly ash on some properties of mortar and notably suppressing alkali-silica reac-tion," *Revista de la Construccion*, vol. 22, no. 2, pp. 419–430, 2023, doi: 10.7764/RDLC.22.2.419.
25. R. Jurczak and F. Szmatuła, "Evaluation of the possibility of replacing fly ash with glass powder in lower-strength concrete mixes," *Applied Sciences (Switzerland)*, vol. 11, no. 1, pp. 1–10, Jan. 2021, doi: 10.3390/app11010396.
26. A. R. Boccaccini, M. Bficker, J. Bossert2, and K. Marszalek, "Glass matrix composites from coal flyash and waste glass," 1997.
27. M. Erol, S. Küçükbayrak, and A. Ersoy-Meriçboyu, "The recycling of the coal fly ash in glass production," in *Journal of Environmental Science and Health - Part A Toxic/Hazardous Substances and Environmental Engineering*, Sep. 2006, pp. 1921–1929. doi: 10.1080/10934520600779208.
28. E. S. Sunarsih, G. W. Patanti, R. S. Agustin, and K. Rahmawati, "Utilization of Waste Glass and Fly Ash as a Replacement of Material Concrete," in *IOP Conference Series: Earth and Environmental Science*, IOP Publishing Ltd., Mar. 2021. doi: 10.1088/1742-6596/1808/1/012004.
29. G. Ludwik. Golewski, "Assessing of water absorption on concrete composites containing fly ash up to 30% in regards to structures completely immersed in water," *Case Studies in Construction Materials* , vol. 19, no. e02337., 2023.
30. S. N. Ghosh and S. K. Handoo, "Infrared and Raman spectral studies in cement and concrete (review)," *Cem Concr Res*, vol. 10, no. 6, pp. 771–782, 1980, doi: 10.1016/0008-8846(80)90005-8.
31. M. O. Yusuf, "Bond Characterization in Cementitious Material Binders Using Fourier-Transform Infrared Spectroscopy," *Applied Sciences*, vol. 13, no. 5, p. 3353, Mar. 2023, doi: 10.3390/app13053353.